Dchs1-Fat4 Regulation of Runx2 Activity

Zein, Mohamed Ahmed Ragab

Awarding institution:
King's College London

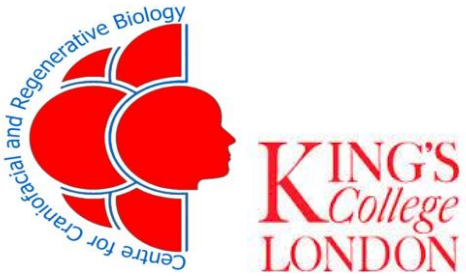

MSC IN REGENERATIVE DENTISTRY

2018/19

7NNYRD03

Laboratory Project in Regenerative Dentistry

DCHS1-FAT4 REGULATION OF RUNX2 ACTIVITY

Supervised by Prof. Philippa Francis-West

MOHAMED ZEIN

1544959

A report submitted in partial fulfilment of the requirements for the degree of MSc in Regenerative Dentistry

Submitted July 2019

King's College University of London

Faculty of Dentistry, Oral & Craniofacial Sciences

Abstract

Bones have multiple embryonic origins and form following two main pathways, intramembranous or endochondral ossifications. Bone development is therefore a complex process that can be affected by multiple diseases such as van Maldergem syndrome, characterized mainly by craniofacial abnormalities. This syndrome is caused by loss of function mutations in FAT4 and DCHS1 genes in humans. The Dchs1-Fat4 signalling pathway is crucial for embryonic development in both mice and humans and is heavily involved in osteoblast differentiation in mice. Deregulation of this pathway leads to major craniofacial defects. In this study, we take a closer look at Dchs1-Fat4 regulation of the activity and expression levels of the master regulator of osteoblast differentiation, Runx2, and its direct targets, including Spp1, Mmp9, and Alpl, by qPCR and Western Blot. We first show that the expression of Osteopontin (Spp1) is regulated by Fat4. The expression of Mmp9 and Alpl genes seems to be negatively regulated by Fat4 and positively regulated by Dchs1. Then we show that Fat4 knockdown has no effect on Runx2 RNA levels, but decreases its protein levels, suggesting that Fat4 differentially regulates Runx2 expression. We therefore suggest a new mechanism of action for Fat4, in which it directly regulates Runx2 activity, without mediation from hippo pathway effectors Yap and Taz.

TABLE OF CONTENTS

Background and Introduction **4**

Overview *4*

Embryonic Origin of Bone *4*

Intramembranous Bone Formation *5*

Endochondral Bone Formation *5*

Control and Regulation of Bone Development *7*

Runx2 ..... *8*

Regulation of Runx2 Activity *9*

Van Maldergem Syndrome *10*

Dchs1-Fat4 Pathway *11*

Dchs1-Fat4 regulation of Osteogenesis *12*

Dchs1-Fat4 regulation of Yap/Taz *13*

Hypothesis and Aims **15**

Materials and Methods **18**

Results: **21**

Conclusion and Discussion: **31**

References **36**

Acknowledgements **41**

Appendices **42**

Primer Validation: *42*

BACKGROUND AND INTRODUCTION

OVERVIEW

Our bones help us move, give us shape and support our body, and they keep developing until the early twenties for most females, and around the age of eighteen for most males. Bone development or ossification is a complex process that starts by the 6th - 7th week of embryonic life. Our bones differ in a lot of aspects as seen in Fig 1, such as shape, size, embryonic origin, and also in terms of susceptibility to diseases, as some of them may be more vulnerable to diseases, such as osteoporosis, than others.

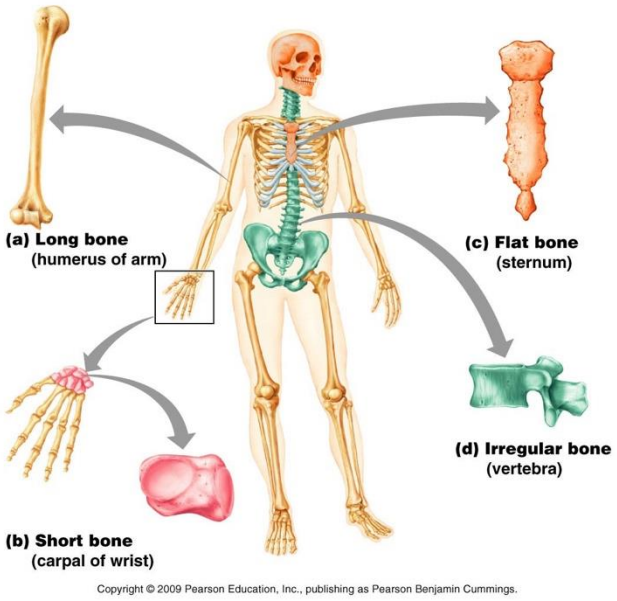

Fig 1: Classification of Bones.

Different types, shapes, and sizes of bones in the body

EMBRYONIC ORIGIN OF BONE

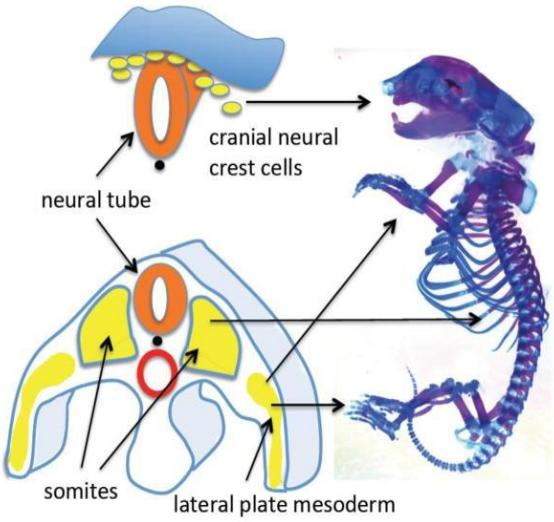

Fig 2: Diagram showing contribution of cranial neural crest, paraxial and lateral plate mesoderm cells to formation of mouse skeleton.

(*Berendsen and Olsen., 2015*)

Three different embryonic lineages generate the skeleton (*Gilbert SF, 2000*):

- The paraxial mesoderm (somites) generates the axial skeleton,
- The lateral plate mesoderm generates the limb skeleton,
- And cranial neural crest generates the majority of craniofacial bones and cartilage. (NB: some of the cranial bones are derived from unsegmented mesoderm.)

Multiple cell types are involved in the bone development and the shaping process. ***Osteoblasts***, which are the cells that make bone, are derived from mesenchymal stem cells, and ***osteoclasts***, which are the cells that resorb bone, are derived from hematopoietic stem cells. The osteoblasts mediate the differentiation of osteoclasts. Once the osteoblasts are finished making bone, they are incorporated in the bone matrix and then turn into ***osteocytes***, the most abundant cell type in bone (*Katsimbri,* 2017), which act as mechano-sensors of bone and have further functions in bone formation and development (*Aarden et al., 1994*).

There are two major osteogenic pathways: ***intramembranous ossification*** and ***endochondral ossification***.

INTRAMEMBRANOUS BONE FORMATION

Intramembranous ossification is the direct conversion of mesenchymal cells into bone. This pathway, which is demonstrated in Fig 3, occurs mainly in the bones of skull and face, where the neural crest- or mesoderm-derived mesenchymal stem cells proliferate and gather together to then differentiate into specialized cells: some develop into capillaries, and others into osteoblasts (*Gilbert SF, 2000*). The osteogenic cells in the surrounding connective tissue then differentiate into new osteoblasts.

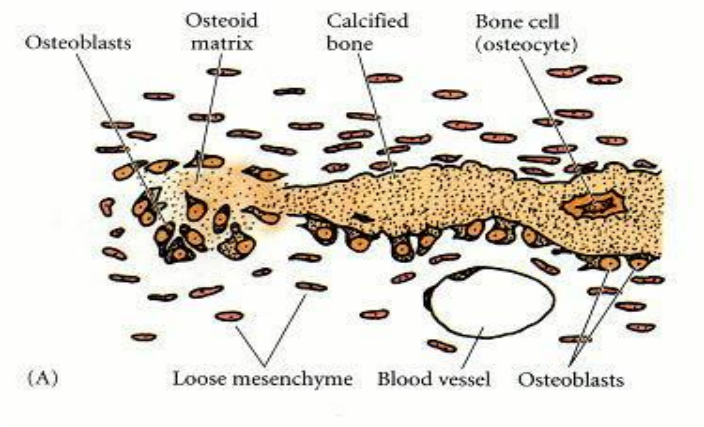

Fig 3: Diagram of intramembranous ossification.

Mesenchymal stem cells gather to differentiate into osteoblasts that deposit osteoid matrix, they then align along the matrix. Some of these osteoblasts later become osteocytes.

(*Gilbert SF, 2000*)

ENDOCHONDRAL BONE FORMATION

Endochondral ossification is the process by which mesenchymal cells differentiate into chondrocytes to form cartilage tissue, which is then replaced by bone cells (*Horton, 1990*). This pathway, detailed in Fig 4, is mainly responsible for formation of bones of the axial and appendicular skeleton (limbs) (*Maes and*

Kronenberg, 2016) and usually takes longer than the intramembranous pathway to make bone. The start is similar to the intramembranous pathway, where mesenchymal cells gather at bone formation sites. But in this case, cells differentiate into chondrocytes instead of osteoblasts (Fig 4a) and synthesize a special type of extra-cellular matrix (ECM), thus creating a cartilaginous model (Fig 4b). Then the perichondrium, a cartilage-covering membrane, appears. The cartilaginous model grows as more matrix is produced. The cartilage is then replaced by bone, with two mechanisms believed to be in action. First, the mechanism previously established as the most common one regarding the fate of the hypertrophic chondrocytes, is their death following the calcification of the cartilaginous matrix, due to lack of nutrients reaching them, and the invasion of the space left empty following their death by blood vessels which carry the osteogenic cells that later differentiate into osteoblasts, which then start forming bone matrix. But more recent studies regarding the fate of chondrocytes suggest that these cells are able to transform directly into osteoblasts, or bone-making cells (*Tsang et al. 2015*). Studies used the Cre-ERt2 LoxP system, a very powerful genetic cell lineage tracing method to determine the fate of chondrocytes (*Hinton et al., 2017*). These studies found that hypertrophic chondrocytes expressing a fluorescent reporter had a molecular resemblance to osteoblasts in terms of expressing bone markers, suggesting that the phenomenon of the direct transformation of the chondrocytes into bone cells is a fairly common event. And although some hypertrophic chondrocytes undergo apoptosis, most of them express high levels of BCL2, an anti-apoptotic protein. Moreover, BrdU experiments have shown that some hypertrophic chondrocytes undergo the process of cell division (*Jing et al., 2015*), suggesting that these cells seem like active cells that express bone markers.

Two or three months into foetal life, ossification increases to create the defined primary ossification centre, the place where ossification has initiated (Fig 4c). After birth, the secondary ossification centres form at the ends of bone (Fig 4e) to leave a small cartilage zone, the growth plate, where the bone continues to grow in length.

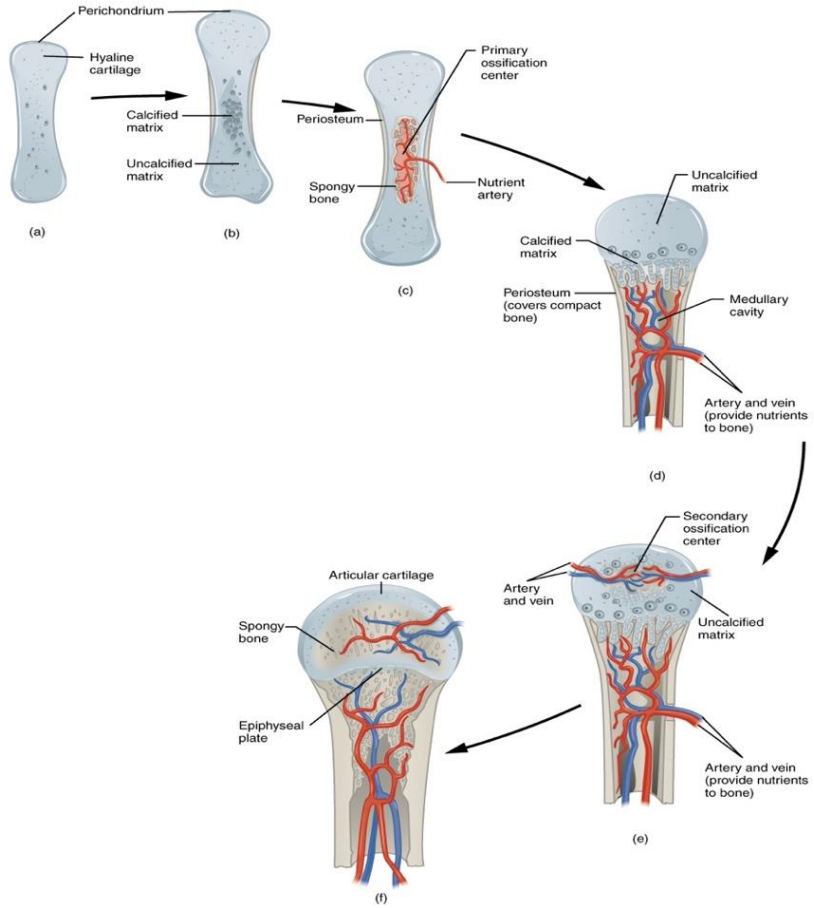

Fig 4: Diagram of endochondral ossification

(a) Mesenchymal cells differentiate into chondrocytes.
(b) Formation of the cartilaginous model and the perichondrium
(c) Capillaries invade the cartilage and formation of primary ossification centre
(d) Cartilage and chondrocytes grow at ends of bone.
(e) Development of secondary ossification centres
(f) Cartilage stays at epiphysial or growth plate or as articular cartilage

(*OpenStax, Anatomy & Physiology. OpenStax CNX. Feb 26, 2016*)

CONTROL AND REGULATION OF BONE DEVELOPMENT

Multiple factors control bone growth, such as cell-cell interactions, transcription factors such as Runx2 and Osterix, growth factors such as IGF (Insulin-like growth factor), and mechanical forces (*Solheim, 1998*). Defects in growth occur in, for example, osteogenesis imperfects, also known as brittle bone disease (Van Dijk et al., 2011). Bone maintenance can also be altered by diseases such as Paget's disease, osteoporosis (affects osteoclasts), osteosclerosis (affects osteoblasts) (*Roselló-Díez and Joyner, 2015*). Other growth factors such as members of the TGFβ superfamily and BMPs (Bone morphogenetic proteins) regulate bone shape (*Solheim, 1998*).

Endochondral ossification is regulated by multiple pathways and molecules such as Wnts, Hedgehog, and Notch (*Hojo et al., 2015*). These molecules and signalling pathways interact with each other to coordinate multiple processes such as osteoblast and chondrocyte proliferation and differentiation. Moreover, in the endochondral pathway, BMP signalling induces Sox9, a transcription factor

required for commitment of undifferentiated mesenchymal stem cells into chondrocytes.

RUNX2

The main protagonist of osteoblast differentiation is **Runx2** (Runt-related transcription factor 2), the master transcription factor for osteogenesis. Runx2 is known to act as a protein that binds specific DNA sequences within target genes and influence their transcription either positively or negatively (*Latchman, 1997*). The crucial role of Runx2 in osteoblast differentiation and ossification was first reported in 1997, as mice with Runx2 mutations died right after birth and showed absence of bone formation and ossification (*Otto et al., 1997*). As shown in Fig 5, Runx2 is involved at every stage of the osteoblast differentiation process, but its activity and specificity are regulated by expression of co-activators/co-repressors, and the levels of Runx2 expression. Runx2 also regulates the expression of multiple osteoblast marker genes such as Osteocalcin, osterix, and p21, through *cis*-acting element found in the promoters of these genes and is sufficient to induce expression of multiple osteoblast marker genes in non-osteoblastic cells (*Bruderer et al., 2014*). All of this is evidence that Runx2 is the master regulator for osteoblast differentiation.

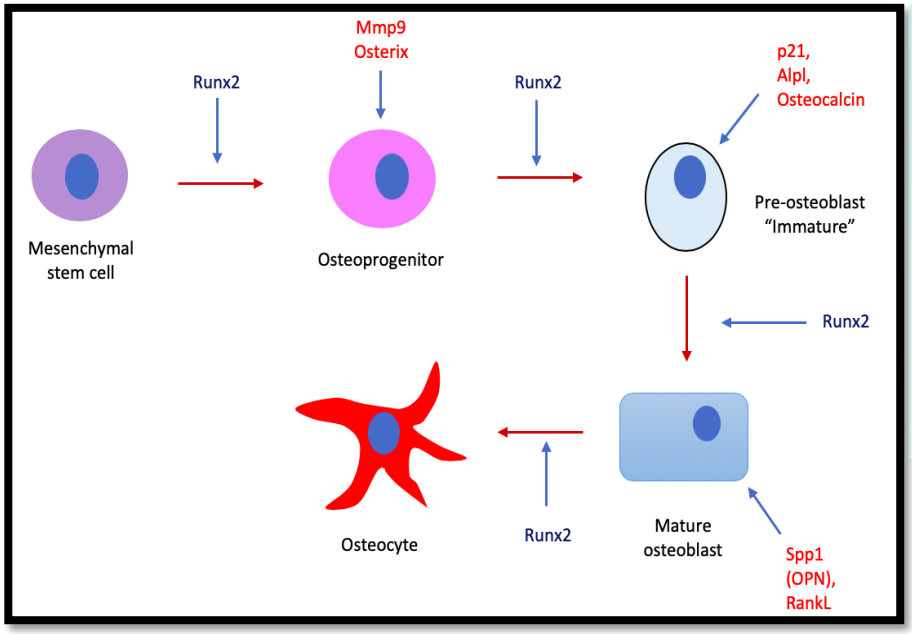

Fig 5: Diagram showing the involvement of Runx2 in osteoblast differentiation. Genes in red are also involved in the differentiation process and are direct targets of Runx2.

Yoshida et al. in 2004 have shown that Runx2$^{-/-}$ deficient mice completely lack chondrocyte maturation, concluding that the transcription factor is also essential for chondrocyte maturation in the endochondral pathway.

REGULATION OF RUNX2 ACTIVITY

In 2001, *Shirakabe et al.* found that Runx2 activity was regulated by two homebox genes: Msx2 and Dlx5. Msx2 represses the transcription activity of Runx2 by interacting with it, and Dlx5 has an activity which interferes with the ability of Msx2 to interact with Runx2 and also repress the transcriptional activity of Runx2 itself. Runx2 is also a key binding partner of Yap/Taz, two effectors of the hippo pathway which control organ size and regeneration (*Seo et al., 2013*), and there is evidence that Yap/Taz modulate the activity of Runx2. Taz can potentiate activity of Runx2 upon binding to promote osteoblast differentiation, while inhibiting PPARγ, which controls adipocyte fate (*Cui et al., 2003*; *Pan et al.,2018*). On the other hand, Yap can inhibit Runx2 function by blocking its transcriptional activity, therefore inhibiting its ability to activate specific transcriptional targets such as TGFβ1 receptor and Osteocalcin (*Zaidi et al., 2004*).

All of the genes in red colour in the diagram in Fig 5 are proven to be direct targets of Runx2, such as Mmp9, Alpl (Alkaline Phosphatase), Spp1 (Osteopontin), and RankL, and they are all present and expressed at different stages of osteoblast differentiation. Moreover, the expression of some of these differentiation-related genes (Osteopontin and Osteocalcin) is reduced by overexpression of Yap1 (*Seo et al., 2013*).

It has also been shown that Runx2 activity is positively regulated upon phosphorylation in human bone marrow stromal cells (*Shui et al., 2003*), and that phosphorylation of the transcription factor regulates its transactivation potential of Osteocalcin. The MAPK pathway can either positively or negatively regulate bone development through phosphorylation of Runx2 (*Vimalraj et al., 2015*; *Ge et al., 2007; Huang et al., 2012*), therefore affecting Runx2 activity. With Runx2 comprising multiple phosphorylation sites, it can be positively- or negatively-regulated depending on the phosphorylated amino acid residues (*Bruderer et al., 2014*).

Runx2 is also implicated in the cell cycle, as an increase in expression was detected during the slow cell cycle proliferation (G0 phase), and a decrease during the rapid proliferation, and that Runx2 expression is also reduced in G1/S transition, G2 and M phases of the cell cycle, but then increases after mitosis (M) (*Galindo et al., 2005*).

VAN MALDERGEM SYNDROME

Multiple diseases and injuries of the bones are major causes of abnormalities of the human skeletal system. Some of these diseases have a genetic basis, such as cerebro-facio-articular syndrome, known as **van Maldergem syndrome**. First described in 1992, it is a rare condition characterized by limb abnormalities, conductive hearing loss due to malformations in the outer ear (Fig 6 g-l) and middle ear, intellectual disabilities, susceptibility in bone fractures and craniofacial malformations such as hypertelorism (widening of the face) (Fig 6 a-f) (*Mansour et al., 2012*).

Fig 6: Facial characteristics of van Maldergem syndrome.

- a-f: The faces of the patients are characterized by maxillary hypoplasia (flat face), broad nasal bridge, telecanthus (increased distance between medial canthi of the eyes), blepharophimosis (horizontally narrow palpebral fissure).
- g-i: ear malformations of VMS patients. There is superior and inferior helical folds, microtia (underdeveloped pinna), which leads to atresia of the external auditory meatus with conductive hearing loss.

(*Mansour et al., 2012*)

Cappello et al. reported in 2013 that loss of funtion mutations in the genes encoding the proto-cadherins **DCHS1 and FAT4**, which act as a receptor-ligand pair, lead to the recessive van Maldergem syndrome.

DCHS1-FAT4 PATHWAY

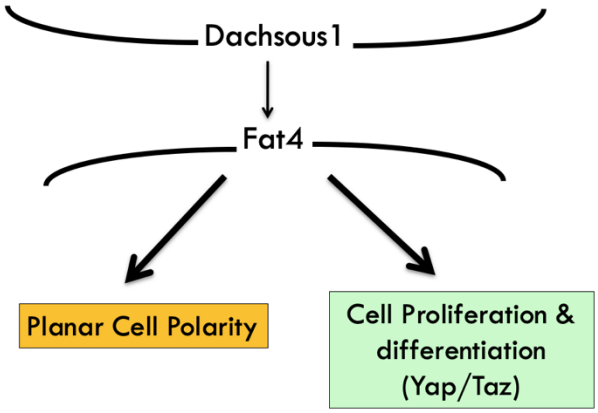

Fig 7: Diagram showing the role of Dchs1-Fat4

The importance of these proto-cadherins in embryonic development in both mice and humans (*Kuta et al., 2016*) makes it imperative for us to understand the mechanisms behind this signalling pathway, and also the mechanisms behind its deregulation leads to major developmental diseases, made me choose it as one of the focus of my research project. μ-CT scans of $Fat4^{-/-}$ and $Dchs1^{-/-}$ mouse skull cap revealed significantly smaller bones and enlarged fontanelles (Fig 8), indicating a delay in mineralization.

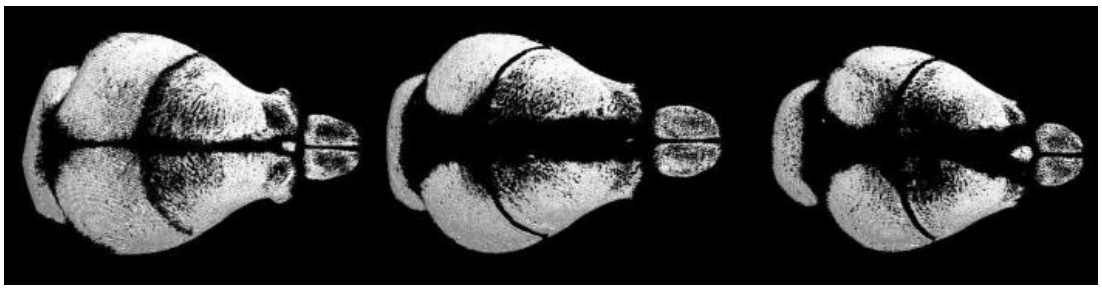

WT $Dchs1^{-/-}$ $Fat4^{-/-}$

Fig 8: μ-CT scans of WT, $Fat4^{-/-}$ and $Dchs1^{-/-}$ skull cap of P0 pups.

All bones analysed are significantly smaller in mutants, which results in a smaller face and larger fontanelles.

(*Crespo-Enriquez et al., in press*)

Fat4 and Dchs1 are the vertebrate homologues of *Drosophila* Fat and Ds, which regulate planar cell polarity, the coordinated alignment of cell polarity across a tissue plane. Comparison between Fat4-Dchs1 and their *Drosophila* homologues have given insight into the way these proto-cadherins function in vertebrates. Strong evidence that planar cell polarity regulation is conserved in mammals and vertebrates (*Mao et al., 2016*) includes Fat regulation of PCP in kidneys as $Fat4^{-/-}$ mutants show defects in orientated cell divisions in the extending kidney tubules (*Saburi et al., 2008*).

DCHS1-FAT4 REGULATION OF OSTEOGENESIS

It is also established that one of the key roles of Dchs1-Fat4 signalling is within the early Runx2-positive osteogenic progenitors. And preliminary work has shown that Runx2 reporters (6XOSE, p21 and TgfβR1) are regulated by Dchs1-Fat4 signalling (Fig 9), and that these reporters are differentially regulated by Yap/Taz.

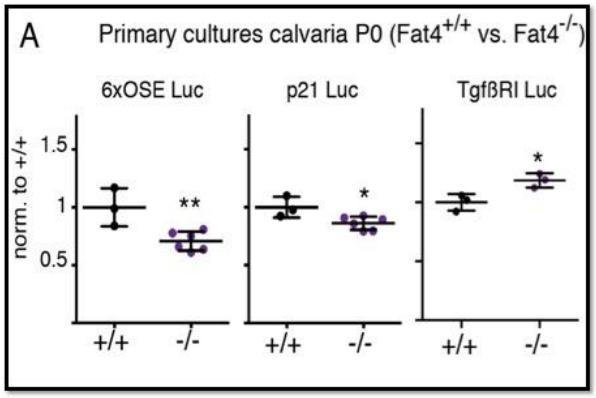

Fig 9: Runx2 reporters (6xOSE, p21 and TgfβR1) are regulated by Fat4 in calvaria P0 bones in Fat4 mutants.

Fat4 mutants show significant changes compared to WT mice in Runx2 reporters activity. Unpaired two-tailed Student's t-test for comparison of each sample with control. Significance: *P≤0.05, **P≤0.01, ns=not significant).

(*Crespo-Enriquez et al., in press*)

Recent studies also show that absence of Dchs1-Fat4 signalling leads to over-proliferation and expansion of osteoblast precursors, as shown in Fig 10 by immunostaining of osteogenic expressing progenitors Runx2 and Osterix. Moreover, *Dchs1*$^{-/-}$ embryos showed significantly smaller domain of calcein labelling in frontal and parietal bones, suggesting that these mutant embryos have delayed mineralization and osteoblast differentiation (Fig 11).

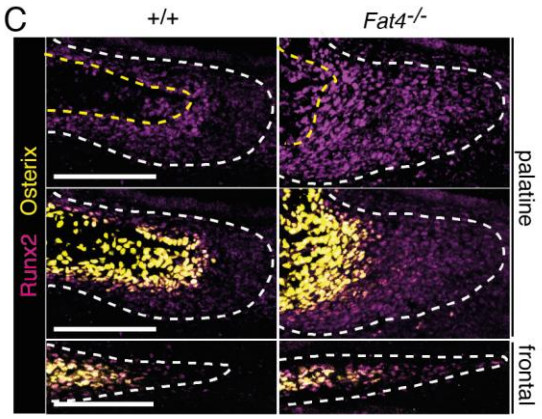

Fig 10: Fat4 and Dchs1 regulate the number of osteoblast progenitors

Osteogenic fronts of frontal and palatine bones in WT and *Fat4*$^{-/-}$ mutants showing Runx2 (magenta) and Osterix (yellow) immunostaining.

We see an expansion of Runx2^{+ve} and Osterix^{-ve} (osteogenic progenitors) in palatine and calvaria bones.

(*Crespo-Enriquez et al., in press*)

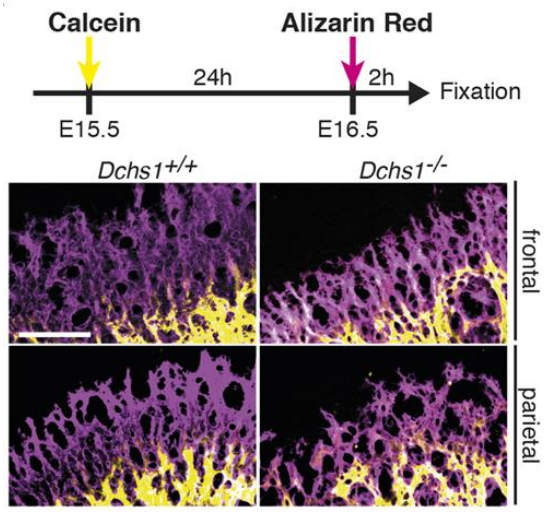

Fig 11: Sequential Calcein (yellow) and Alizarin red (magenta) labelling of E16.5 osteogenic fronts in WT and *Dchs1*$^{-/-}$ frontal and parietal bones

The domain of calcein labelling in *Dchs1*$^{-/-}$ mutants is significantly smaller compared to WT.

(*Crespo-Enriquez et al., in press*)

DCHS1-FAT4 REGULATION OF YAP/TAZ

In *Drosophila*, Fat and Ds inhibit tissue growth by inhibiting the Hippo pathway, which regulates the activity of Yorkie (homologue of Yap) to control cell proliferation, survival and differentiation (*Misra and Irvine, 2018*) (Fig 7). Dchs1-Fat4 also regulate the activity of **Yap**, a homologue of transcriptional co-factor Yorkie in the developing brain, heart and within the osteoblast progenitors. However, distinct mechanisms have evolved for Fat4 regulation of Yap in vertebrates that do not involve hippo kinases.

Yap (yes-associated protein) and its paralogue **Taz**, a transcriptional co-activator with PDZ-binding motif, also control organ size through regulation of cell proliferation and apoptosis (*Yu and Guan, 2013*). They can act as both transcriptional co-activators and repressors.

In mammals, Fat4 regulation of Yap is implicated in the cerebral cortex as loss of Dchs1 and Fat4 was related to increased neuronal proliferation and nuclear Yap/Taz activity. Key transcriptional binding partners of Yap/Taz include **TEADs** (1-4), and the analysis of Yap/TEAD targets revealed that they act at both enhancer and promoter sites (*Galli et al., 2015*). Recent research also suggests that Yap and Taz can regulate transcription through distinct mechanisms and can have independent roles even in the same cell (*Sun et al., 2017*).

Preliminary work includes luciferase reporter assays looking at the effect of Yap and Taz expression knockdown on the activity of Runx2 reporters (6xOSE, p21 and TgfβR1) in both WT (Fig 12B) and Fat4$^{-/-}$ (Fig 12C) osteoblasts. This study

revealed that Yap knockdown significantly decreased activity of Runx2- TgfβR1 reporter in both WT and Fat4 mutants (Fig 12B-C) but had no effect on the other reporters. Taz knockdown studies resulted in decreased activity of 6xOSE and p21 reporters in WT osteoblasts (Fig 12B) but had no effect on these reporters in Fat4 mutants (Fig 12C), suggesting that the activity of Taz-Runx2 complexes is decreased in Fat4$^{-/-}$ mutant osteoblasts. This data highlights the differential role of Yap and Taz in osteoblasts.

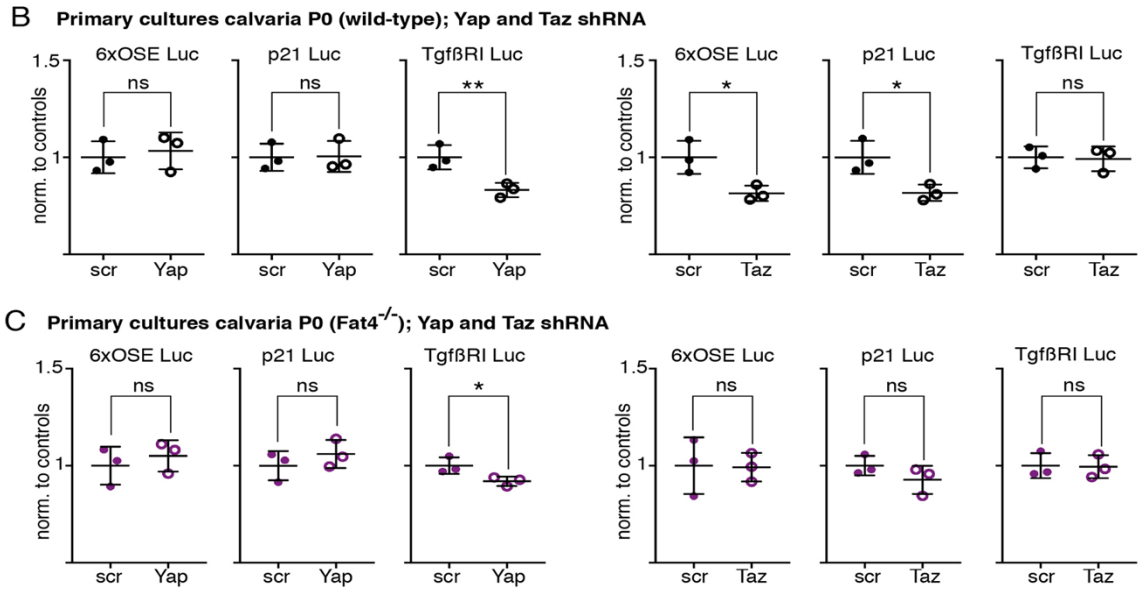

Fig 12: The effect of knockdown of Yap and Taz expression by Yap and Taz shRNA constructs on the activity of three Runx2 reporters (6xOSE, p21, and TgfβR1) in WT (B) and *Fat4*$^{-/-}$ (C) osteoblasts from primary cultures calvaria P0. (scr = scrambled shRNA plasmid).

(*Crespo-Enriquez et al., in press*)

HYPOTHESIS AND AIMS

Preliminary work:

- **RNAseq:**

Preliminary work in the laboratory included an RNAseq study that was done to advance our understanding of how Dchs1-Fat4 signalling regulates osteoblast differentiation. The analysis was from parietal and frontal bones of both *Fat4*$^{-/-}$ mutants and wild-type E16.5 embryos. The reason why two types of bones were used is because they have distinct embryonic origins and their development is regulated by different signalling networks (*Quarto et al., 2009*), therefore comparing the two types will allow us to identify the main regulators of Dchs1-Fat4 signalling in osteoblasts.

More than 120 significantly differentially expressed genes were identified in the study, with over 2-fold change in expression between mutants and wild-types, with about 50% of these genes downregulated in the mutants.

Collectively, the RNAseq analyses identified:

a) A subgroup of Yap-targets, and
b) Multiple differentially-regulated genes known to be involved in osteoblast development, including Runx2 targets Mmp9, Osteopontin (Spp1), Alpl (Alkaline phosphatase) and RankL.

It is worth mentioning that the RNAseq started from a mixed population of cells from bone of WT versus mutants, which means that not all the cells were mature and fully developed osteoblasts, so there were cells of all stages of the differentiation process. This makes it impossible to conclude that all differentially expressed genes are direct targets of Fat4 or Dchs1. So, some of these differentially expressed genes in the RNAseq may reflect differences in number of progenitors versus the more differentiated osteoblasts i.e. changes in expression are secondary to changes in ratio of progenitors to osteoblasts.

Table 1: Runx2 candidate direct targets and their fold-change in expression:

Gene	Log2 fold change
Mmp9	-1.61
Spp1 (Osteopontin)	-0.64
Alpl (Alkaline phosphatase)	-0.47
RankL	-1.27

My project looks at the regulation of the activity of Runx2 and its targets (listed in Table 1) by the Dchs1/Fat4 signalling pathway.

We hypothesize that alterations in Dchs1-Fat4 signalling pathway alter Runx2 activity in part by Yap and Taz.

My strategy to validate this hypothesis is detailed in the flowchart below:

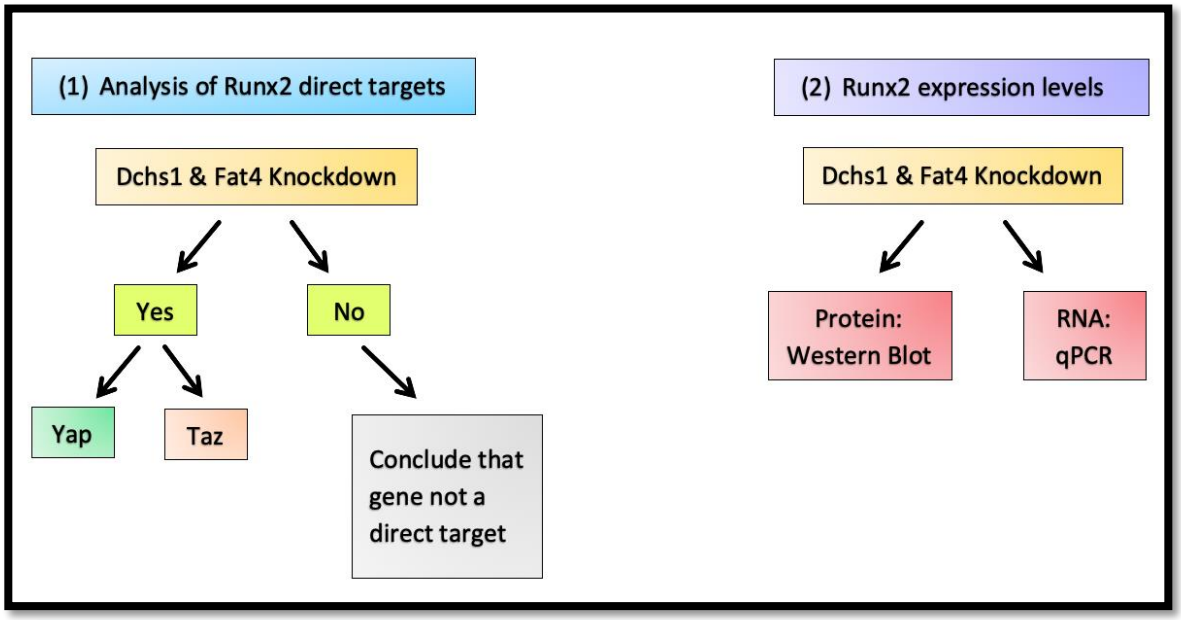

Fig 13: Flowchart detailing strategy and individual aims of research project.

Our primary aim is to determine which Runx2 direct targets are regulated by the Dchs1-Fat4 signalling pathway, and if they are differentially regulated by Yap and Taz.

To validate this hypothesis, we will:

1. Analyse Runx2 direct targets by knocking-down Dchs1 and/or Fat4. If gene expression of the targets is changed following the knockdown, then we can investigate the role of Yap and Taz in the regulation of these targets. If gene expression is not altered by Dchs1-Fat4 knockdown, then we can conclude that these genes are not direct targets of Dchs1-Fat4.
2. Analyse Runx2 levels of expression as altered Runx2 levels could contribute to delayed osteogenesis. We will again knock-down Dchs1-Fat4, and look at Runx2 protein levels by Western Blot, and RNA levels via qPCR.

MATERIALS AND METHODS

- **Cell culture: RNA and luciferase transfections**

Mouse osteoblast cell line MC3T3-E1 (ATCC® CRL-2593™) were used. Cells were seeded at a density of $6{,}0x10^4$ cells per well in 24-well plates (one plate for RNA and one plate for luciferase) in growth media (Gibco®, cat.no. 10270-106, 2mM L-glutamine, AB/AM). 24 hours later, cells were transfected with 250ng of siRNA and/or shRNA in "RNA" plate, and with 250ng of reporter plasmid together with 50ng of Renilla plasmid in "luciferase" plate using Lipofectamine® LTX with Plus™ Reagent kit (Invitrogen®, cat. no. 15338-100) conforming to manufacturer instructions. Renilla plasmid was used as internal control to standardize transfection efficiency for the "luciferase" assays.

Alternatively, cells were seeded at a density of $1{,}2x10^5$ then 24 hours later, they were transfected with 250 siRNA vectors using Lipofectamine RNAiMAX Reagent (Invitrogen®, cat. no. 13778-150). Then 24 hours later, cells were transfected with remaining vectors (250ng of shRNA vectors and/or 250ng of reporter plasmid with 50ng of Renilla plasmid) using Lipofectamine® LTX with Plus™ Reagent kit (Invitrogen®, cat. no. 15338-100).

RNA was extracted from cultured cells 48 hours after transfections using RNeasy Micro Kit (Qiagen). Luciferase reporter assays were carried out with Dual-Luciferase® Reporter (DLR™) Assay System (Promega®, cat. no. E1910) 48 hours following lipofection; 2 technical replicates per experiment were measured and averaged.

  - Plasmids: Yap-Tead luciferase reporter, and its control reporter (Schlegelmilch et al., 2011). Taz (Wwtr1) NM_133784, TRCN0000095951; Yap (Yap1) NM_009534), TRCN0000238432; Dchs1 NM_001162943, TRCN0000341730 and Fat4 NM_024582, TRCN0000055983 were obtained from MISSION® shRNA library (Sigma). Dchs1, Fat4 or control siRNA (Cappello et al., 2013).

- **cDNA preparation and qPCR:**

Extracted RNA was reverse transcribed to cDNAs (100ng) with GoScript Kit (Promega). Quantitative PCR was carried out using Fast Start SYBR Green Master

(Roche) on a BioRad CFX 384 (BioRad) machine. Relative gene expression was quantified by standard curve and delta-delta methods using B2M as a control housekeeping gene.

Table 2: Primers sequences

Gene	**Primer sequence**
B2M	Forward: CTGCTACGTAACACAGTTCCACCC
	Reverse: CATGATGCTTGATCACATGTCTCG
Mmp9	Forward: TGAATCAGCTGGCTTTTGTG
	Reverse: GTGGATAGCTCGGTGGTGTT
RankL	Forward: AGCCGAGACTACGGCAAGTA
	Reverse: GCGCTCGAAAGTACAGGAAC
Spp1	Forward: AAAGGGCAGCCATGAGTCAA
	Reverse: CAGGCTGGCTTTGGAACTTG
Alpl	Forward: CCAGCAGGTTTCTCTCTTGG
	Reverse: CTGGGAGTCTCATCCTGAGC
p21	Forward: GCCTTAGCCCTCACTCTGTG
	Reverse: AGGGCCCTACCGTCCTACTA
Runx2	Forward: ACCGAGACCAACCGAGTCAGT
	Reverse: ACACGGTGTCACTGCGCTGAA
Fat4	Forward: AGGACTTTGGTGGCATTGAG
	Reverse: GGGTCTGTTTTGGAGATGGA
Osteocalcin	Forward: CATGAGGACCCTCTCTCTGC
	Reverse: TGGACATGAAGGCTTTGTCA

- **Western Blot analysis:**

Western blot analysis was carried out on total proteins extracted from cell cultures (MC3T3 E1) 48h after transfection with Control siRNA, or Fat4 siRNA, or Fat4 siRNA + Yap shRNA or Fat4 siRNA + Taz shRNA, using Passive Lysis 5X buffer (Promega E194A). Protein concentration was measured at 560nm using a

BCA protein assay kit (Novagen 71258) according to manufacturer's recommendations. 10μg of lysates prepared in Laemmli Buffer (Biorad 1610747) were boiled at 95°C for 5 minutes and then resolved by SDS-PAGE. Proteins were transferred onto PDVF membranes using a Trans-blot Turbo transfer system (Biorad) and blocked with 5% non-fat milk for 1 hour at room temperature. Membranes were incubated overnight at 4°C with the primary antibodies anti-Runx2 (1:1000, Santa Cruz Biotech. Sc-390351) and anti-Cyclophillin B, the loading control (1:1000, R&D MAB5410) followed by incubation with the anti-mouse HRP-conjugated secondary antibody (1:2000, Dako). Proteins of interest were detected with an ECL substrate (Biorad 1705060) and imaged with Chemidoc Imaging system (Biorad). Densitometric analysis was carried out using ImageJ software and the signal of the protein of interest was normalised to the loading control.

- **Statistical analysis:**

To compare and standardise the results, the value for controls from each experiment was normalised to 1. The remaining experimental values were then standardized to the control value of 1. All stated numbers (n) are for different biological replicates (*in vitro*). All biological replicates from were then analysed collectively as one using Prism 8 GraphPad. For the cell culture experiments, at least two technical replicates were analysed, and the average was used. The significance of the data was determined using un-paired Students t-test comparing control with experimental values. Within the graphs, the control bar combines the individual control values from each data set. Sample size, n=1-3.

RESULTS:

I. Osteopontin (Spp1) is a target of Fat4.

I first designed two primers for each candidate Runx2 direct target listed in Table 1. We then validated these primers by qPCR to determine the best primer sequence to use for each gene, checking to see if they elicit a proper response and also to determine the optimal concentration for each primer sequence. Concentrations of 300nM, 400nM, and 500nM were tested. The primer validation also allows us to obtain a standard curve value, which is later on used in the analysis of the qPCR results. Based on primer validation data, we used a concentration of 300nM for the Spp1 and Alpl genes, and a concentration of 500nM for the Mmp9 and RankL genes.

I then proceeded to perform qPCRs to determine which genes are regulated by Dchs1-Fat4. I used cDNA that was previously prepared by other lab members. The samples we used were control, Dchs1 shRNA and Fat4 shRNA constructs. Technical replicates were done for each sample. B2M was used as a housekeeping gene (300nM concentration).

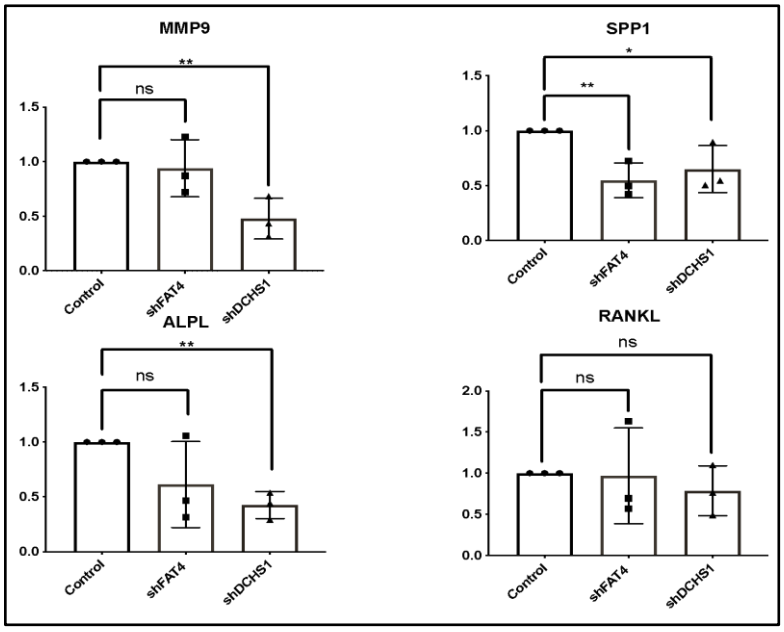

Fig 14: qPCR analysis of RNA levels of Runx2 direct targets following knockdown of Dchs1 and Fat4 by shRNA constructs, compared with Control samples.

Data points indicate each independent biological experiment (n=3), each experiment had 2 technical replicates. Each control value from each experiment was standardized to 1. Statistical analysis: Unpaired two-tailed Student's t-test for comparison of each sample with control. Significance: *P≤0.05, **P≤0.01, ns=not significant).

Analysis of the results was done by the standard curve method.

The results were conclusive for the Spp1 experiments, where we see a significant downregulation of Spp1 expression in Fat4 shRNA- and Dchs1 shRNA-treated cells compared to the control sample, showing that knockdown of Fat4 and

Dchs1 decreases expression levels of Spp1. The results for the other genes were inconclusive/statistically insignificant. The triplicate values for each sample from each experiment were quite variable, making it hard to conclude/interpret these results. An interesting aspect of these results is the effect on Dchs1 shRNA-treated cells on the expression of the Alpl and Mmp9 genes. We can see a clear and significant downregulation in the expression of these genes when treated with Dchs1 shRNA, but not Fat4 shRNA, suggesting that Dchs1 and Fat4 might be acting in a different way in these two genes, and also that some genes like Spp1 might be more sensitive to the loss of Fat4 than others.

As RankL expression is not altered by either Dchs1 or Fat4, we concluded that RankL was not a direct target of Dchs1-Fat4 and decided to drop it from future analyses.

II. Positive controls

In the next experiments, I focused on Fat4 and its regulation of the Runx2 targets. I also started using siRNA constructs instead of shRNA, because many results from the previous experiments using shRNA constructs were not conclusive, and other lab members were simultaneously using siRNA constructs and obtaining good results.

I also started used Yap and Taz shRNA constructs to monitor Yap and Taz activity and looking at the combined effect of Fat4, Yap and Taz knockdowns.

I first transfected MC3T3-E1 cells (osteoblast cell line) at a density of around 60,000 cells per well with control siRNA, Fat4 siRNA, Fat4 siRNA + Yap shRNA, and Fat4 siRNA + Taz shRNA constructs.

- Luciferase assay:

Dchs1-Fat4 normally repress/inhibit the activity of Yap-Taz/Tead, which means that if we knockdown Fat4 or Dchs1, we expect Yap and Taz activity to increase. And if we knock down Yap and Taz, we expect the activity of their reporters to increase. To validate this model and as a positive control for the experiments, I had a separate luciferase plate with cells transfected at the same density with the same vectors, plus Yap luciferase reporter and Renilla luciferase reporter. Two wells were transfected per sample as technical replicates. Three biological

replicates were done. RNA and luciferase were extracted 48 hours after transfections.

A dual-luciferase reporter assay was then done to look at the activities of both the firefly luciferase reporter (contained in the Yap luciferase reporter) and the Renilla luciferase. Analyses (Fig 15) revealed that Fat4 knockdown decreased Yap and Taz reporter activity, and knockdown of Yap shRNA and Taz shRNA had no effect. These results contradict the predicted ones. Our results were also very variable, impeding us from making any conclusions.

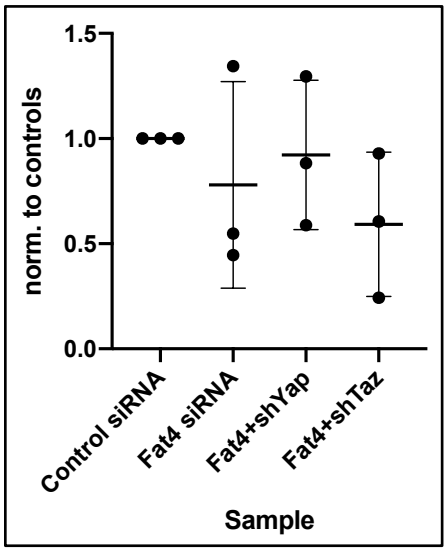

Fig 15: Dual-luciferase assay results

MC3T3-E1 cells treated with Control and Fat4 siRNA, Fat4 siRNA + Yap shRNA, Fat4 siRNA + Taz shRNA, and Yap luciferase and Renilla Luciferase reporters

Data points indicate each independent biological experiment (n=3), each experiment had 2 technical replicates. Each control value from each experiment was standardized to 1.

I then performed a qPCR to again look at the Fat4 regulation of the Runx2 targets and also Yap and Taz regulation of these genes. I added more Runx2 targets (shown in Fig 5) to the analysis: Osteocalcin, Fat4 and p21. The last two are used as positive controls as we would expect Fat4 siRNA to knock down the Fat4 RNA levels, and p21 is a verified target of Fat4 according to preliminary work, where knockdown of Fat4 led to a decrease in p21 expression. B2M was again used as a housekeeping gene.

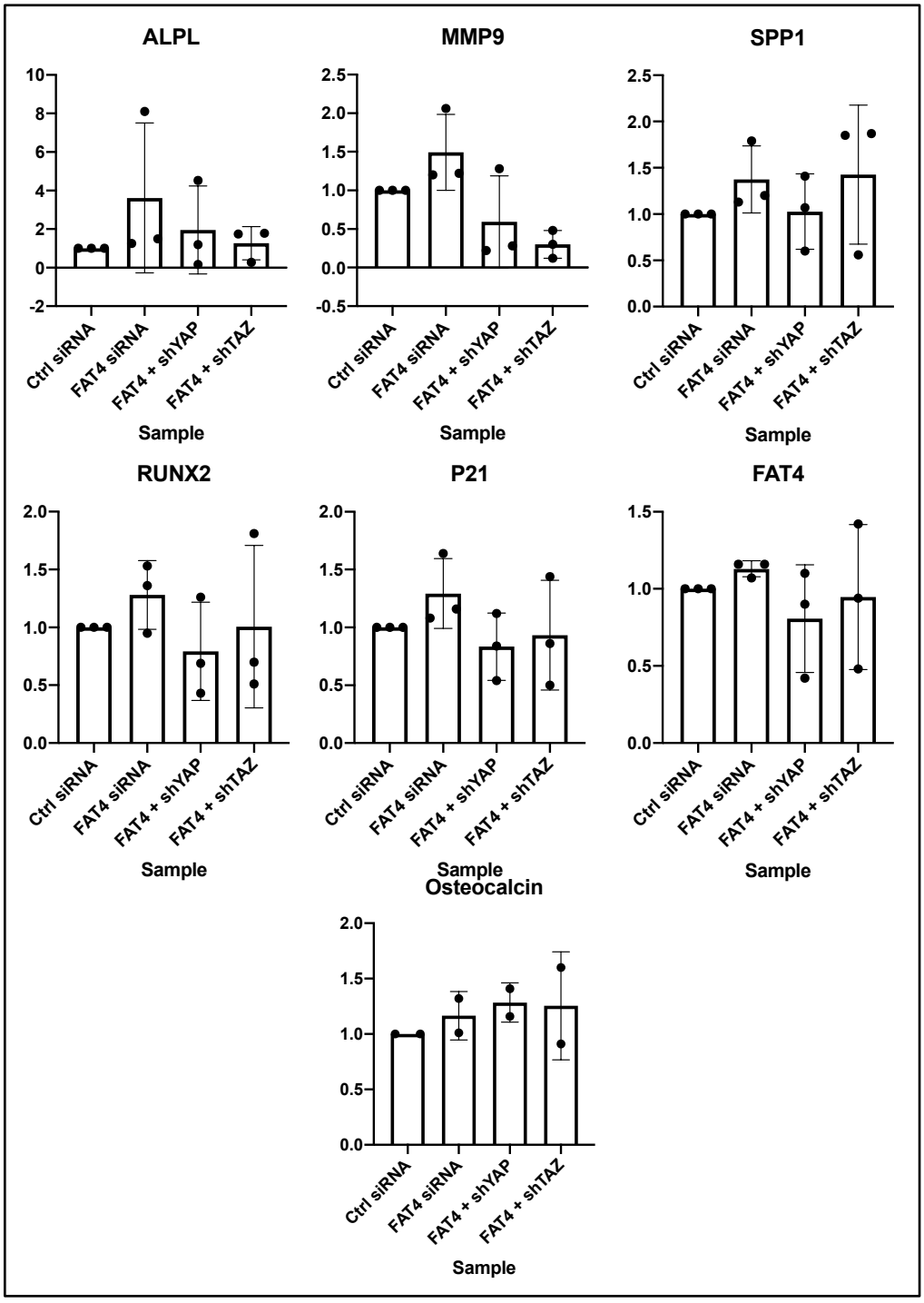

Fig 16: qPCR analysis of RNA levels of Runx2 targets Alpl, Mmp9, Spp1 (Osteopontin), p21, and osteocalcin, and Runx2 and Fat4 genes, with Fat4, Yap and Taz knockdown.

Data points indicate each independent biological experiment (n=3), each experiment had 2 technical replicates. Each control value from each experiment was standardized to 1.

As we can see in the analysis in Fig 16, there was no significant change in expression of all the genes analysed following Fat4 knockdown. Fat4 upregulation in Spp1 contradicts our previous results (Fig 14). Fat4 knockdown also lead to an increase in p21 expression, contradicting preliminary work done in the lab. We also see an upregulation of Fat4 siRNA in the Fat4 gene, which does not make sense. There is also a big variability in the results, especially the Yap and Taz knockdowns, preventing us from making any conclusions.

Therefore, the results from luciferase assays and Fat4 RNA experiments showed that our assays were not working as predicted.

Results III:

Following discussions with the project supervisor, I decided to double the cell density for the next set of transfections, with 120,000 cells per well instead of 60,000. We believed that cell density could have been a factor in the variability and inconclusiveness of the results. Another issue we believed could have been a factor was transfection efficiency. We thought that a low percentage of our cells were successfully transfected with and expressing our constructs. Therefore, we decided to add additional wells with cells seeded at same density (120,000), but which were transfected with GFP (green fluorescent protein). This will allow us to determine the transfection efficiency by taking pictures of the GFP-transfected cells 24 hours and 48 hours following the transfections and counting them.

I also followed an alternative transfection protocol, tested and validated by other members of the lab. I used the same vectors and constructs, but instead of transfecting the cells with all the vectors on the same day (protocol used for previous transfections), I did the transfections in stages:

- 24 hours following cell seeding at indicated density, I transfected the cells with the Control siRNA and Fat4 siRNA constructs using the Lipofectamine RNAiMAX reagent (instead of Lipofectamine LTX with Plus reagent), specified for transfections using RNAi constructs.
- Then, 24 hours after transfecting the cells with the siRNA constructs, I transfected them with the remaining constructs (Yap shRNA and TAZ shRNA, and Yap luciferase and Renilla luciferase for the luciferase plate). RNA and luciferase extracted 48 hours after primary transfections (siRNA).

Due to time constrictions, we could only do the experiments once (n=1).

Dual-luciferase assay revealed that Fat4 knockdown decreased Yap and Taz reporter activity (Fig 17), indicating that our knockdown assays were working as predicted.

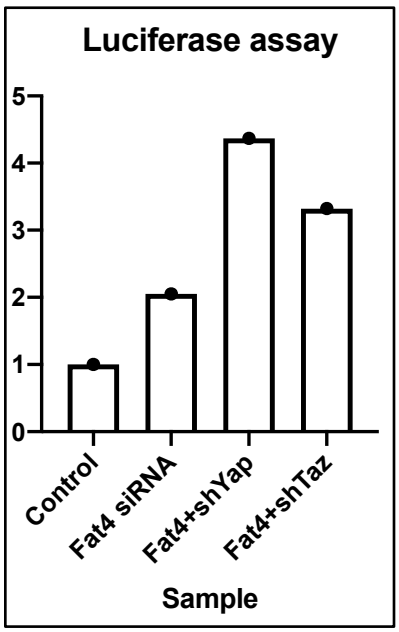

Fig 17: Dual-luciferase assay results

Data points indicate each independent biological experiment (n=3), each experiment had 2 technical replicates. Each control value from each experiment was standardized to 1.

I then performed a qPCR experiment, to look at the expression of the same genes from the previous experiment (Fig 16).

What we saw in the results (Fig 18) is that Fat4 gene expression was decreased following Fat4 knockdown, meaning that our positive controls were working. Although, p21 expression did not change after knocking down Fat4 (it decreased in preliminary work), we deduced that since the experiments were done by different plating densities, it might lead to different results. Spp1 expression was also decreased following Fat4 knockdown, consistent with previous results (Fig 14). Alpl, Mmp9, and osteocalcin expression increased with Fat4 knockdown, suggesting that these three genes may be negatively regulated by Fat4, as regulation of gene expression can be either positive or negative.

Yap and Taz knockdown led to decreased expression of all genes analysed, which may suggest that these genes are regulated by Yap/Taz. And for genes like Mmp9 and Alpl, we see a differential decrease of Yap and Taz expression, which suggests that these genes are differentially regulated by Yap and Taz. However, analysis of Yap/Taz-Tead reporter showed the activity was increased in Yap and Taz shRNA – treated cells, indicating that the assay had not worked as expected.

Despite the conclusiveness of most of the results regarding gene expression following Fat4 knockdown, it was hard to make any conclusions on Yap and Taz expression (except for Mmp9 and Alpl) as their results did not make much sense.

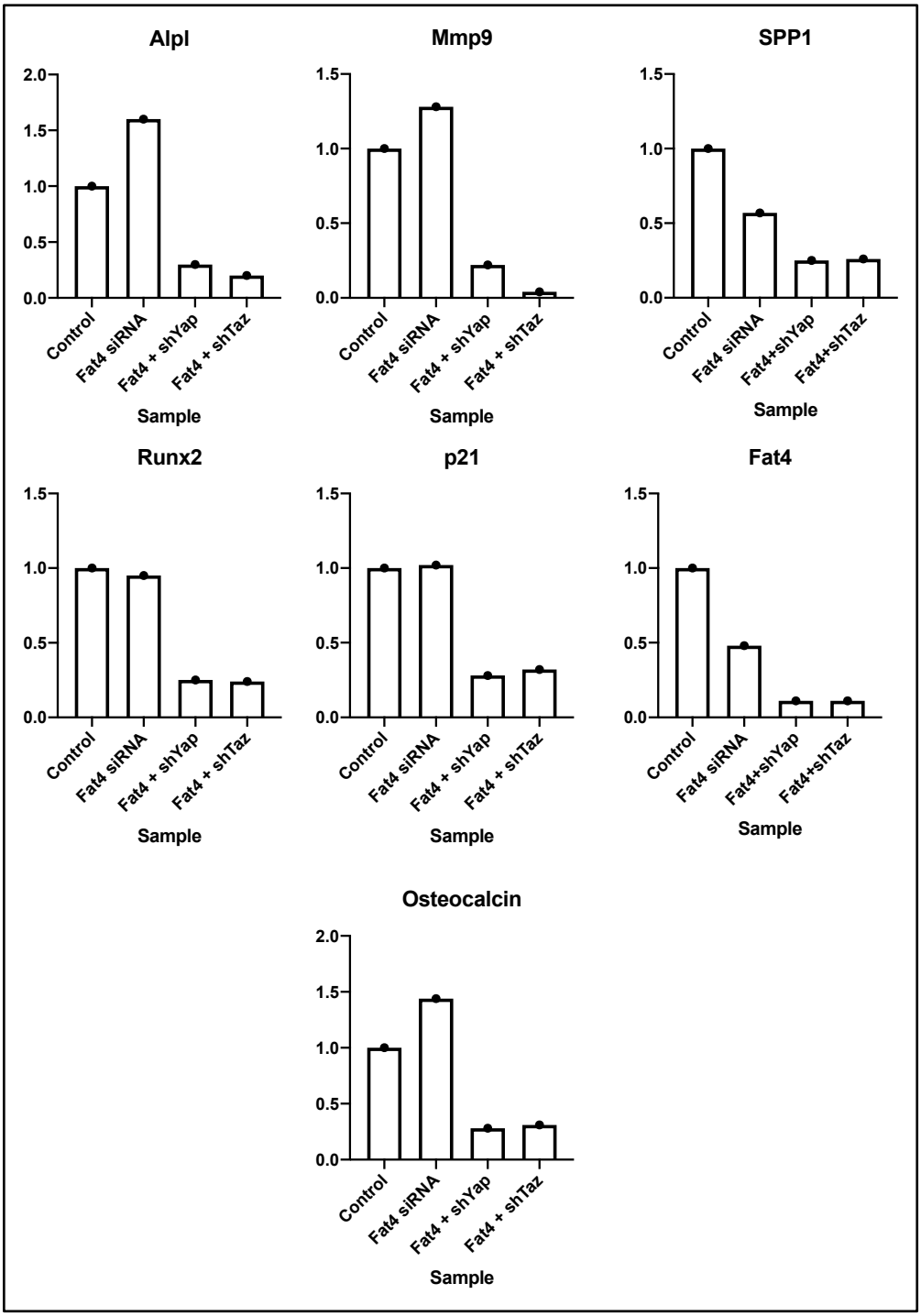

Fig 18: qPCR analysis of RNA levels of Runx2 targets Alpl, Mmp9, Spp1 (Osteopontin), p21, and osteocalcin, and Runx2 and Fat4 genes, with Fat4, Yap and Taz knockdown.

Data points indicate each independent biological experiment (n=1), each experiment had 2 technical replicates. Each control value from each experiment was standardized to 1.

Transfection efficiency: GFP expression

Although results from this experiment were more conclusive than previous ones and gave us more insight into Fat4 regulation of the expression of Runx2 and its targets, the GFP expression experiments (Fig 19) confirmed our concerns that transfection efficiency was indeed an issue that may have been affecting our results.

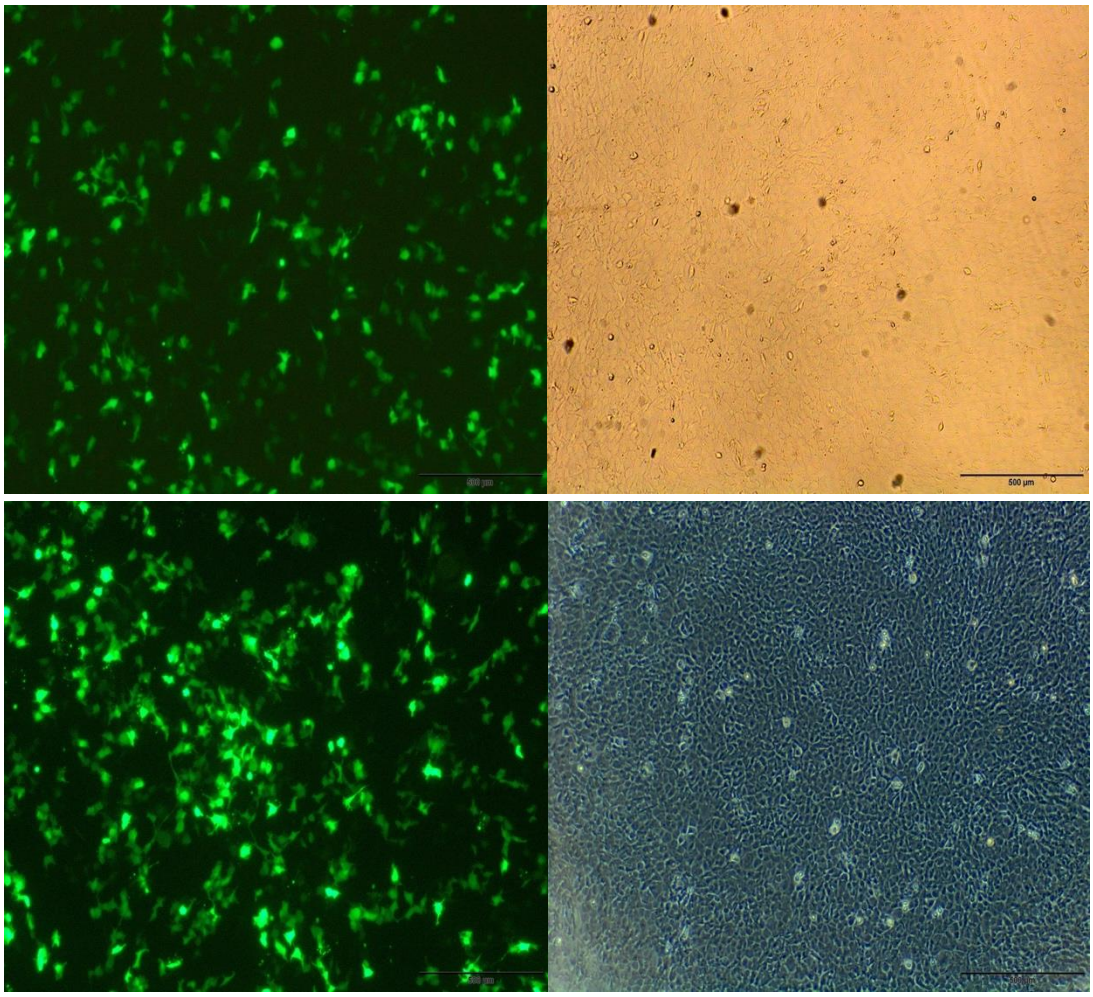

Fig 19: Photographs of GFP-transfected MC3T3-E1 obtained with fluorescent microscope.

Cells were observed under bright-field view (right) and fluorescence view (left) (20X magnification). Upper row photographs taken 24h after transfections and lower row photographs taken 48h after transfections.

Cell counting of photographs above revealed that 24 hours following GFP transfections, only around 33% of the cells were expressing GFP, and 48 hours after transfections, approximately 49% of the cells were expressing GFP. It is important to note that this difference in percentage of GFP-expressing cells between 24 hours and 48 hours does not necessarily mean that during that 24 hour period, 16% of our cells started expressing GFP, as cells expressing GFP in the first 24 hours can express more GFP and be more fluorescent in the next 24 hours, making it look like more cells are expressing GFP and affecting our cell counting analysis.

Runx2 levels of expression:

I also included the Runx2 gene in the analysis, to look at Runx2 RNA levels., to see if changes in Runx2 expression contribute to changes in expression of Runx2 targets. qPCR analysis (Fig 20) revealed that Runx2 RNA levels do not change significantly following Fat4 knockdown, but RNA levels of targets (Spp1) do, suggesting that changes in Runx2 RNA levels do not contribute to changes in targets RNA levels.

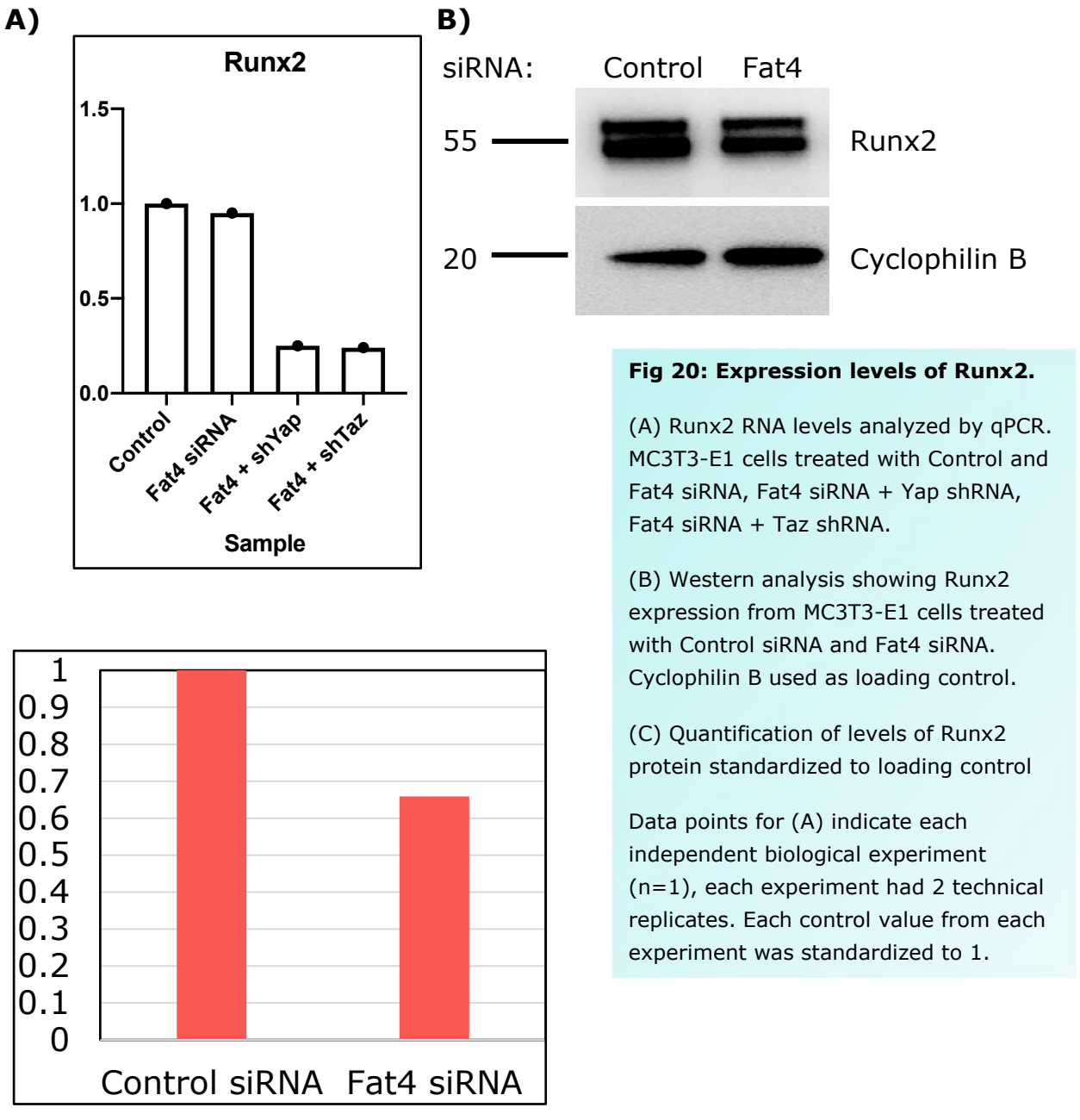

Fig 20: Expression levels of Runx2.

(A) Runx2 RNA levels analyzed by qPCR. MC3T3-E1 cells treated with Control and Fat4 siRNA, Fat4 siRNA + Yap shRNA, Fat4 siRNA + Taz shRNA.

(B) Western analysis showing Runx2 expression from MC3T3-E1 cells treated with Control siRNA and Fat4 siRNA. Cyclophilin B used as loading control.

(C) Quantification of levels of Runx2 protein standardized to loading control

Data points for (A) indicate each independent biological experiment (n=1), each experiment had 2 technical replicates. Each control value from each experiment was standardized to 1.

I then went on to analyse Runx2 protein levels by Western Blot using a Runx2 antibody. This was done to examine how Fat4 knockdown affects Runx2 levels and whether we would see changes in protein levels, or if they would remain unchanged like RNA levels. As we can see in the analysis in Fig 20, knockdown of Fat4 decreased Runx2 expression and protein levels.

CONCLUSION AND DISCUSSION:

To conclude our study, we verified one Runx2 direct target as a Fat4 target: Spp1. This gene codes for the osteopontin protein, a major non-collagenous protein (NCP) involved in bone matrix organization and deposition (*Bailey et al., 2017*). Recent knockout studies have also revealed that the osteopontin protein acts alongside other NCPs such as osteocalcin to maintain bone strength in bone matrix (*Bailey et al., 2017*). The Spp1 gene itself is a direct target of Runx2, with the expression of the gene being nearly absent in *Runx2*$^{-/-}$ mice, and the transcription factor having the ability to upregulate the expression of the gene (*Komori, 2017*).

The findings of our study are summarized in Fig 21. We found that the expression of Spp1 decreases when Fat4 is knocked down (Fig 14 & 18), meaning that Spp1 is directly regulated by Fat4. Due to variability of some of the results, we could not conclude on the regulation of Yap and Taz and whether they differentially regulate Spp1.

Other investigated genes included Runx2 targets Mmp9 and Alpl. The former is a key regulator of growth plate maturation and bone formation (*Pratap et al., 2005*), and the latter plays an important role in promoting bone mineralization (*Weng and Su, 2013*). Our results showed that the expression of these two genes increases following Fat4 knockdown (Fig 18), revealing that they are negatively regulated by Fat4. But our results also showed that the expression of Mmp9 and Alpl decreases following Dchs1 knockdown (Fig 14), suggesting that Dchs1 regulates Mmp9 and Alpl expression, but not Fat4. This is striking because the phenotypes of Fat4 and Dchs1 are extremely similar (*Kuta et al., 2016; Crespo et al., in press*).

We also concluded that RankL is not regulated by either Fat4 or Dchs1 due to lack of changes in gene expression following knockdown (Fig 14). This is interesting because according to the RNAseq data (Table 1), RankL has a bigger fold-change in expression in *Fat4*$^{-/-}$ mutants compared with the fold-change in Spp1 expression, despite both of these reaching their highest expression levels at the same stage of osteoblast differentiation, late on in mature osteoblasts (Fig 5). This can be explained by the fact that RankL is mostly expressed in high levels in osteoclasts and required for their survival, proliferation and

differentiation. It is also expressed by osteoblasts where the binding of RankL to its receptor Rank triggers differentiation of osteoclast-precursors into osteoclasts (*Park et al., 2017*). Moreover, RankL-deficient mice and patients with *RankL* mutations manifest evident osteoporosis (a disease that affects osteoclasts) and an absence of osteoclasts (*Fumoto et al., 2014*). It has also been reported that during endochondral ossification, RankL expression in osteoblasts at later stages is kept at a relatively low level (*Mori et al., 2006*).

As mentioned earlier, the RNAseq started with a mixed population of cells, meaning that osteoclasts were also part of that population, and could be the reason why we see a significant fold-change in RankL expression in the $Fat4^{-/-}$ mutants is because these mutants are also lacking in Runx2 expression, which directly regulates RankL, and, consistent with this hypothesis, the RNAseq data identified other osteoclast markers with changes in their expression. Therefore, that change in RankL expression in $Fat4^{-/-}$ mutants may be mainly due to decreased Runx2 levels, not Fat4 knockout, and may also be secondary to fewer differentiated osteoblasts. But it is interesting that we found alterations in Spp1 which is expressed at the same stage of osteoblast differentiation, which calls for further investigation into the RNAseq data, and the role and expression of RankL in osteoblast differentiation.

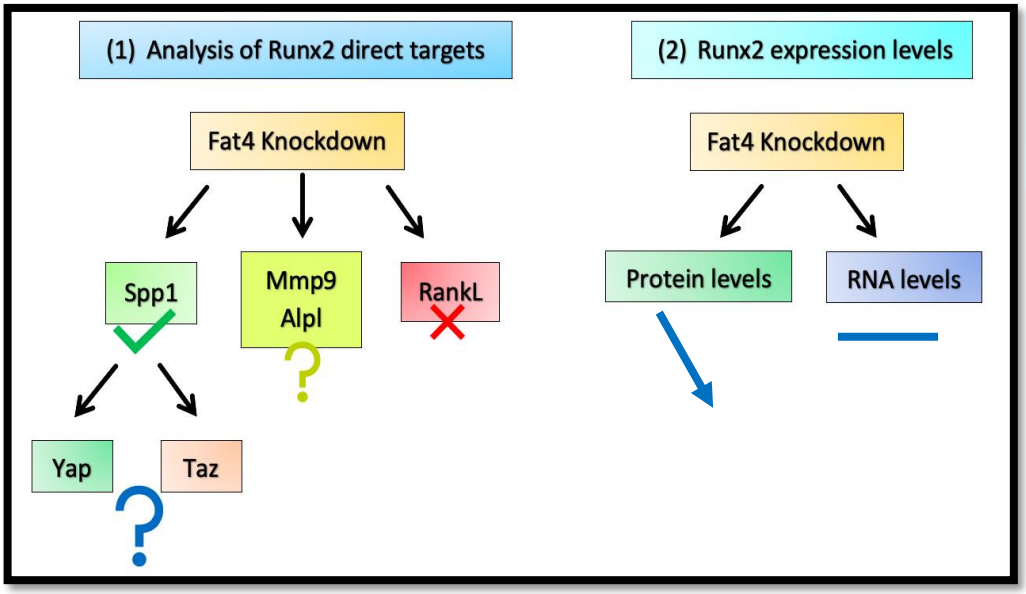

Fig 21: Flowchart summarizing findings of our study.

Analysis of Runx2 expression levels also revealed that following Fat4 knockdown, RNA levels remain unchanged (Fig 18), whereas protein levels are decreased (Fig 20). We can therefore conclude that Fat4 differentially regulates Runx2

expression (altered protein levels but not RNA). I should note that I only had n=1 for these experiments, so they need to be repeated to obtain more reliable results.

Moreover, since RNA levels of Runx2 direct targets such as Spp1 change following Fat4 knockdown, we can also deduce that changes in Runx2 RNA levels of expression do not induce or directly contribute to changes in RNA levels of direct targets, but that changes in protein levels may do so.

Decreased Runx2 expression levels could contribute to decreased rate of osteogenesis and haploinsufficiency (model of dominant gene action in which a single copy of standard allele at a locus in heterozygous combination with a varaint allele in not enough to produce standard phenotype), as the loss of one copy of RUNX2 in humans results in Cleidocranial dysplasia, characterized by enlarged fontanelles (Fig 8).

The established model or mechanism of action of Fat4, shown in Fig 22, is that the protocadherin inhibits/represses activity of Yap/Taz, which then regulate the activity of Runx2, which then regulates the expression of direct targets such as Spp1. But the model we found following analysis of results from our study indicates that Fat4 may also directly regulate Runx2 activity via regulation of Runx2 protein levels, which then regulates expression of Runx2 targets. This suggests thay Yap and Taz regulation may not be essential in regulation of Runx2 and its targets.

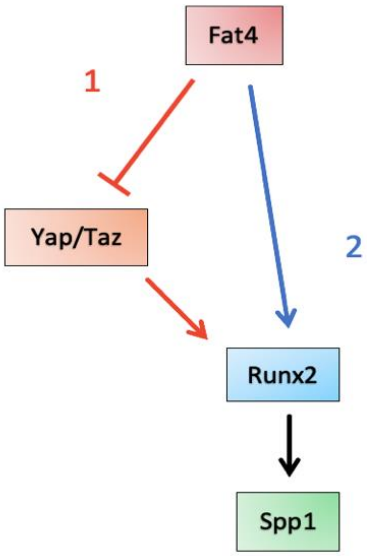

Fig 22: Flowchart showing (1) established model of action of Fat4 and (2) model identified following results from our study

- **Limitations:**

During my research project, I encountered a few issues, with most of them being technical issues that may have influenced our strategy and our study results and analysis. Due to time constrictions and assays not working properly or as predicted, the steps of my work strategy laid out in Fig 13 may not have been done sequentially as desired, but some of them may have been done in parallel.

Technical limitations include transfection efficiency as shown in Fig 19, where GFP expression experiments have shown that less than half of the cells were expressing GFP 48 hours after transfections, indicating that there was also a relatively low percentage of cells expressing our DNA constructs. The efficiency of cell transfection depends on multiple factors such as the cell type, cell health/viability, cell/passage and confluency at time of transfection, the type and amount of molecule transfected, the cell density and the method of transfection. All these factors must be kept in mind and optimized when planning a transfection. Cell density is a particularly interesting factor, because there is not a specific cell density advised for a specific cell line, and also because most protocols advise an incubation period (following transfections) of 48 to 72 hours, despite cell density increasing during that period as cells proliferate. This may also be a problem as we are trying to investigate the immediate effect of the knockdown of a certain molecule, so a 48-hour period may impede that. This may be why Yap/Taz activity was increased in these assays i.e. secondary effects of non-transfected cells which have increased Yap/Taz activity.

Another issue is the variability of the qPCR triplicates. In many of my experiments, the triplicate values in my qPCR analysis were variable, making it hard to interpret the results and averting me from making any conclusions. This variability could be due to human error (pipetting issues…), or the cDNA preparation process, or the cell transfections themselves. Many steps leading up to and during the qPCR must be carried out carefully to avoid variations.

- **Future Directions:**

My research project answered some of my questions, but not all of them, and some aspects of Fat4 and Dchs1 regulation of Runx2 still need to be looked at.

As my results could not reveal the role of Yap/Taz in the regulation of Runx2 and its targets (Fig 18), then I would want to take a closer look at that and investigate it further. I would also do a ChiPseq analysis to identify Yap and Taz dependant genes and look at potential Fat4-Yap and Fat4-Taz targets. I would also do co-precipitation assays to identify Yap-Taz binding partners and see how these complexes are regulated by Dchs1-Fat4 signalling. I may also look to analyse Runx2 co-factors, similarly to targets analysis, and look at their regulation by Dchs1-Fat4 and Yap/Taz.

REFERENCES

1. Gilbert SF. Osteogenesis: the development of bones. In: Developmental Biology 6th Edition. Sunderland (MA): Sinauer Associates; 2000.
2. Berendsen AD, Olsen BR. HHS Public Access. 2016;118(24):6072–8.
3. Katsimbri P. The biology of normal bone remodelling. Eur J Cancer Care (Engl). 2017;26(6):1–5.
4. Aarden, E. M., Nijweide, P. J. and Burger EH. Function of osteocytes in bone. J Cell Biochem. 1994;(55):287–99.
5. Horton WA. The biology of bone growth. Growth Genet Horm. 1990;6(2):1–3.
6. Christa Maes and Henry M. Kronenberg. Chapter 60 - Bone Development and Remodelling. In: J. Larry Jameson, Leslie J De Groot, David M. de Kretser, Linda C. Giudice, Ashley B. Grossman, Shlomo Melmed, John T. Potts, Gordon C. Weir, editor. Endocrinology: Adult and Pediatric (Seventh Edition). 7th ed. W.B. Saunders; 2016. p. 1038–62.
7. Tsang KY, Chan D, Cheah KSE. Fate of growth plate hypertrophic chondrocytes: Death or lineage extension? Dev Growth Differ. 2015;57(2):179–92.
8. Hinton RJ, Jing Y, Jing J, Feng JQ. Roles of Chondrocytes in Endochondral Bone Formation and Fracture Repair. J Dent Res. 2017;96(1):23–30.
9. Jing Y, Zhou X, Han X, Jing J, Von Der Mark K, Wang J, et al. Chondrocytes directly transform into bone cells in mandibular condyle growth. J Dent Res. 2015;94(12):1668–75.
10. OpenStax, Anatomy & Physiology. OpenStax CNX. Feb 26, 2016) http://cnx.org/contents/14fb4ad7-39a1-4eee-ab6e-3ef2482e3e22@8.24.
11. Solheim E. Growth factors in bone. Int Orthop. 1998;22(6):410–6.
12. van Dijk FS, Cobben JM, Kariminejad A, Maugeri A, Nikkels PGJ, van Rijn RR, et al. Osteogenesis Imperfecta: A Review with Clinical Examples. Mol Syndromol [Internet]. 2011;2(1):1–20. Available from: http://www.ncbi.nlm.nih.gov/pubmed/22570641%0Ahttp://www.pubmedcentral.nih.gov/articlerender.fcgi?artid=PMC3343766

13. Roselló-Díez, Alberto and ALJ. Regulation of Long Bone Growth in Vertebrates; It Is Time to Catch Up. Endocr Rev. 2015;36(6):646–80.
14. Hojo H, Ohba S, Chung U Il. Signalling pathways regulating the specification and differentiation of the osteoblast lineage. Regen Ther [Internet]. 2015;1:57–62. Available from: http://dx.doi.org/10.1016/j.reth.2014.10.002
15. Latchman DS. Transcription factors: An overview. Int J Biochem Cell Biol [Internet]. 1997 Dec 1 [cited 2019 Jul 5];29(12):1305–12. Available from: https://www.sciencedirect.com/science/article/pii/S135727259700085X
16. Otto, F. , Kanegane, H. and Mundlos S. Mutations in the RUNX2 gene in patients with cleidocranial dysplasia. Hum Mutat. 2002;19:209–16.
17. Bruderer M, Richards RG, Alini M, Stoddart MJ. Role and regulation of runx2 in osteogenesis. Eur Cells Mater. 2014;28:269–86.
18. Yoshida CA, Yamamoto H, Fujita T, Furuichi T, Ito K, Inoue KI, et al. Runx2 and Runx3 are essential for chondrocyte maturation, and Runx2 regulates limb growth through induction of Indian hedgehog. Genes Dev. 2004;18(8):952–63.
19. Shirakabe K, Terasawa K, Miyama K, Shibuya H, Nishida E. Regulation of the activity of the transcription factor Runx2 by two homeobox proteins, Msx2 and Dlx5. Genes to Cells. 2001;6(10):851–6.
20. Seo E, Basu-Roy U, Gunaratne PH, Coarfa C, Lim DS, Basilico C, et al. SOX2 Regulates YAP1 to Maintain Stemness and Determine Cell Fate in the Osteo-Adipo Lineage. Cell Rep [Internet]. 2013;3(6):2075–87. Available from: http://dx.doi.org/10.1016/j.celrep.2013.05.029
21. Cui G, Jun SB, Jin X, Pham MD, Vogel SS, Lovinger DM, et al. Concurrent activation of striatal direct and indirect pathways during action initiation. Nature [Internet]. 2013;494(7436):238–42. Available from: http://dx.doi.org/10.1038/nature11846
22. Pan JX, Xiong L, Zhao K, Zeng P, Wang B, Tang FL, et al. YAP promotes osteogenesis and suppresses adipogenic differentiation by regulating β-catenin signalling. Bone Res [Internet]. 2018;6(1). Available from: http://dx.doi.org/10.1038/s41413-018-0018-7
23. Zaidi S, Hassan MI, Islam A, Ahmad F. The role of key residues in structure, function, and stability of cytochrome-c. Cell Mol Life Sci. 2014;71(2):229–55.

24. Shui C, Spelsberg TC, Riggs BL, Khosla S. Changes in Runx2/Cbfa1 Expression and Activity During Osteoblastic Differentiation of Human Bone Marrow Stromal Cells. :1–21.
25. Vimalraj S, Arumugam B, Miranda PJ, Selvamurugan N. Runx2: Structure, function, and phosphorylation in osteoblast differentiation. Int J Biol Macromol [Internet]. 2015;78:202–8. Available from: http://dx.doi.org/10.1016/j.ijbiomac.2015.04.008
26. Ge C, Xiao G, Jiang D. and skeletal development. 2007;176(5):709–18.
27. Huang YF, Lin JJ, Lin CH, Su Y, Hung SC. c-Jun N-terminal Kinase 1 Negatively Regulates Osteoblastic Differentiation Induced by BMP2 via Phosphorylation of Runx2 at Ser104. J Bone Miner Res. 2012;27(5):1093–105.
28. Galindo M, Pratap J, Young DW, Hovhannisyan H, Im H-J, Choi J-Y, et al. The Bone-specific Expression of Runx2 Oscillates during the Cell Cycle to Support a G1-related Antiproliferative Function in Osteoblasts. J Biol Chem. 2005;21(280):20274–20285.
29. Mansour S, Swinkels M, Terhal PA, Wilson LC, Rich P, Van Maldergem L, et al. Van Maldergem syndrome: Further characterisation and evidence for neuronal migration abnormalities and autosomal recessive inheritance. Eur J Hum Genet [Internet]. 2012;20(10):1024–31. Available from: http://dx.doi.org/10.1038/ejhg.2012.57
30. Cappello S, Gray MJ, Badouel C, Lange S, Einsiedler M, Srour M, et al. Mutations in genes encoding the cadherin receptor-ligand pair DCHS1 and FAT4 disrupt cerebral cortical development. Nat Genet [Internet]. 2013;45(11):1300–10. Available from: http://dx.doi.org/10.1038/ng.2765
31. Kuta A, Mao Y, Martin T, Ferreira de Sousa C, Whiting D, Zakaria S, et al. Fat4-Dchs1 signalling controls cell proliferation in developing vertebrae. Development. 2016;143(13):2367–75.
32. Mao Y, Kuta A, Crespo-Enriquez I, Whiting D, Martin T, Mulvaney J, et al. Dchs1-Fat4 regulation of polarized cell behaviours during skeletal morphogenesis. Nat Commun [Internet]. 2016;7(May):1–10. Available from: http://dx.doi.org/10.1038/ncomms11469
33. Saburi S, Hester I, Fischer E, Pontoglio M, Eremina V, Gessler M, et al. Loss of Fat4 disrupts PCP signalling and oriented cell division and leads to cystic kidney disease. Nat Genet. 2008;40(8):1010–5.

34. Misra JR, Irvine KD. The Hippo Signalling Network and Its Biological Functions. Annu Rev Genet. 2018;52(1):65–87.
35. Yu F, Guan K. Genesdev210773 355..371. 2013;1(2012):1–17. Available from: papers3://publication/doi/10.1101/gad.210773.112
36. Galli G, Carrara M, Yuan W-C, Valdes-Quezada C, Gurung B, Pepe-Mooney B, et al. YAP drives growth by controlling transcriptional pause release from dynamic enhancers. Mol Cell. 2015;60(2):328–337.
37. Sun C, De Mello V, Mohamed A, Ortuste Quiroga HP, Garcia-Munoz A, Al Bloshi A, et al. Common and Distinctive Functions of the Hippo Effectors Taz and Yap in Skeletal Muscle Stem Cell Function. Stem Cells. 2017;35(8):1958–72.
38. Quarto N, Wan DC, Kwan MD, Panetta NJ, Li S, Longaker MT. Origin matters: Differences in embryonic tissue origin and Wnt signalling determine the osteogenic potential and healing capacity of frontal and parietal calvarial bones. J Bone Miner Res. 2010;25(7):1680–94.
39. Bailey S, Karsenty G, Gundberg C, Vashishth D. Osteocalcin and osteopontin influence bone morphology and mechanical properties. Ann N Y Acad Sci. 2017;1409(1):79–84.
40. Yoshida CA, Yamamoto H, Fujita T, Furuichi T, Ito K, Inoue KI, et al. Runx2 and Runx3 are essential for chondrocyte maturation, and Runx2 regulates limb growth through induction of Indian hedgehog. Genes Dev. 2004;18(8):952–63.
41. Komori T. (2017) Roles of Runx2 in Skeletal Development. In: Groner Y., Ito Y., Liu P., Neil J., Speck N., van Wijnen A. (eds) RUNX Proteins in Development and Cancer. Advances in Experimental Medicine and Biology, vol 962. Springer, Singapore
42. Pratap J, Javed A, Languino LR, van Wijnen AJ, Stein JL, Stein GS, et al. The Runx2 osteogenic transcription factor regulates matrix metalloproteinase 9 in bone metastatic cancer cells and controls cell invasion. Mol Cell Biol [Internet]. 2005;25(19):8581–91.
43. Weng JJ, Su Y. Nuclear matrix-targeting of the osteogenic factor Runx2 is essential for its recognition and activation of the alkaline phosphatase gene. Biochim Biophys Acta - Gen Subj [Internet]. 2013;1830(3):2839–52. Available from: http://dx.doi.org/10.1016/j.bbagen.2012.12.021

44. Park JH, Lee NK, Lee SY. Current Understanding of RANK Signaling in Osteoclast Differentiation and Maturation. Mol Cells. 2017;40(10):706–13.
45. Fumoto T, Takeshita S, Ito M, Ikeda K. Physiological functions of osteoblast lineage and T cell-derived RANKL in bone homeostasis. J Bone Miner Res. 2014;29(4):830–42.
46. Mori K, Kitazawa R, Kondo T, Maeda S, Yamaguchi A, Kitazawa S. Modulation of mouse RANKL gene expression by Runx2 and PKA pathway. J Cell Biochem. 2006;98(6):1629–44.

ACKNOWLEDGEMENTS

I would like to express my gratitude to the supervisor of this project, Prof. Philippa Francis-West, and her entire lab/team members, past and present: Erika Cadoni, Guillermo Villagomez-Olea, Jonna Petzold, Tina Hodgson, and Despoina Kesidou. Without their contribution, the completion of this project would not have been possible. I would also like to extend my gratitude to all staff members of the Department of Craniofacial Development and Stem Cell Biology at the 27th floor of Guy's tower, especially Susmitha Rao for her support during this project. And finally, I would also like to thank Dr. Ana Angelova Volponi for her continued support and encouragement for the duration of this project.

APPENDICES

PRIMER VALIDATION:

I validated primers for four different genes for my analysis. The genes were Runx2 targets Alpl, Mmp9, Spp1 and RankL (or Tnfsf11). The validation method I used was through qPCR (method detailed in Materials & Methods section). I tested the different primers at different concentrations (300nM and 500nM) with samples with different concentrations (100%: original sample. 10%: sample diluted from original sample with 1/10 dilution factor (DF). 1%: sample diluted from 10% sample with 1/10 DF. 0.1%: sample diluted from 1% sample with 1/10 DF). Samples were loaded in triplicates. The average of the triplicate values gives us the Cq mean. Variable triplicates (not within 50 copy numbers from other triplicates of sample) were eliminated from analysis. Trendline equation then provides E value. The closer this value is to 100, the better the quality of the primers. We tested two to three primer sequences for each gene and chose the ones with the best E value (closest to 100).

- **Alpl:**

Sample Concentration		Cq mean
100%	2	22.747451
10%	1	29.357900
1%	0	31.751676
0.1%	-1	32.116551
	c	30.518
	m	-3.0501
	E	112.7443833

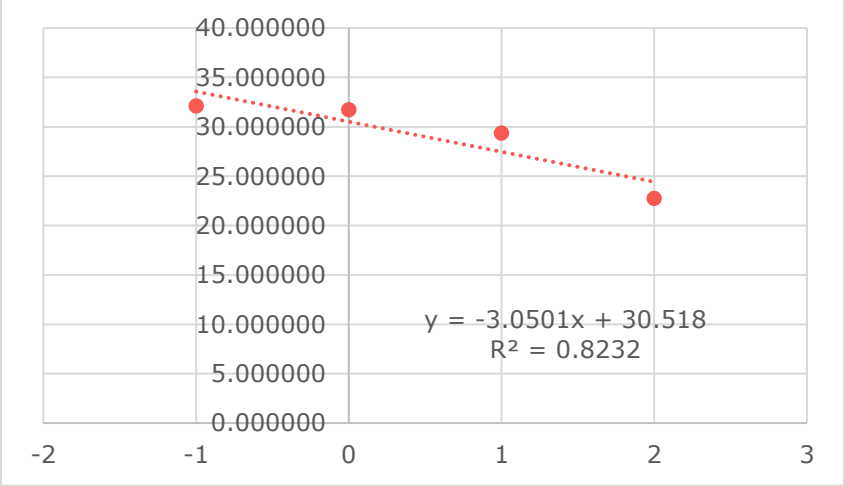

- **Mmp9**

Sample Concentration		Cq mean
100	2	21.475527
10	1	26.889221
1	0	30.139290
0.1	-1	32.416731
	c	29.534
	m	-3.6074
	E	89.32499822

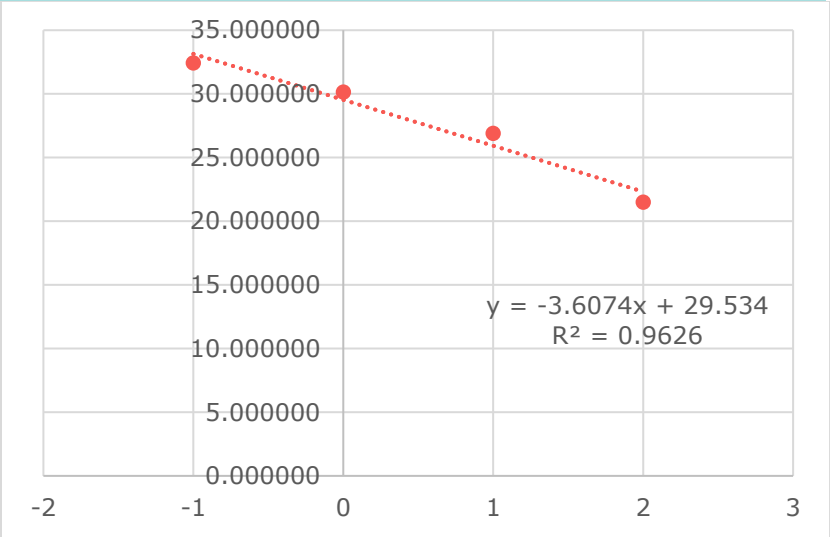

- **Spp1:**

Sample Concentration		Cq mean
100	2	20.710477
10	1	23.538559
1	0	27.463938
0.1	-1	30.432357
	c	27.191
	m	-3.3091
	E	100.5381351

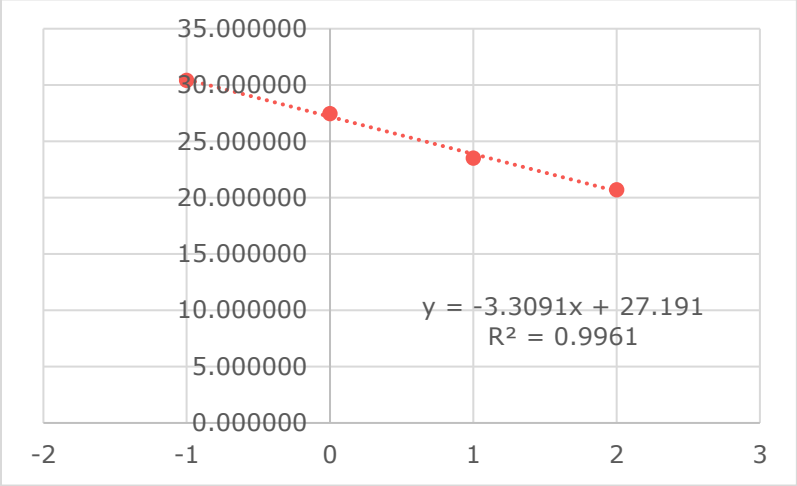

- **RankL (tnfsf11):**

Sample Concentration		Cq mean
100	2	22.217151
10	1	28.568082
1	0	32.962826
0.1	-1	34.882210
	c	31.777
	m	-4.239
	E	72.14907541